

---

EFDA–JET–PR(04)43

P.A. Belo, M.F.F. Nave, T.C. Hender, B. Alper, D. Borba, R.J. Buttery, S. Coda,  
D.F. Howell, M. Maraschek, O. Sauter, F. Serra, E. Westerhof  
and JET EFDA contributors

# Statistical Study of Neo-Classical Tearing Modes Onset on JET



# Statistical Study of Neo-Classical Tearing Modes Onset on JET

P.A. Belo<sup>1</sup>, M.F.F. Nave<sup>1</sup>, T.C. Hender<sup>2</sup>, B. Alper<sup>2</sup>, D. Borba<sup>1</sup>, R.J. Buttery<sup>2</sup>,  
S. Coda<sup>3</sup>, D.F. Howell<sup>2</sup>, M. Maraschek<sup>4</sup>, O. Sauter<sup>5</sup>, F. Serra<sup>1</sup>, E. Westerhof<sup>3</sup>  
and JET EFDA contributors\*

<sup>1</sup>*Associação EURATOM/IST, Centro de Fusão Nuclear, 1049-001 Lisbon, Portugal*

<sup>2</sup>*EURATOM/UKAEA Fusion Association, Culham Science Centre, Abingdon, Oxon. OX14 3DB, UK*

<sup>3</sup>*FOM-Rijnhuizen, Ass. EURATOM-FOM, TEC, PO Box 1207, 3430 BE Nieuwegein, Netherlands*

<sup>4</sup>*Max-Planck-Institut für Plasmaphysik, IPP-EURATOM Assoziation, Boltzmann-Str.2, D-85748 Garching, Germany*

<sup>5</sup>*Centre de Recherches en Physique des Plasmas, Association EURATOM-Switzerland, EPFL 1015 Lausanne, Switzerland*

\* *See annex of J. Pamela et al, "Overview of Recent JET Results and Future Perspectives", Fusion Energy 2002 (Proc. 19<sup>th</sup> IAEA Fusion Energy Conference, Lyon (2002)).*

“This document is intended for publication in the open literature. It is made available on the understanding that it may not be further circulated and extracts or references may not be published prior to publication of the original when applicable, or without the consent of the Publications Officer, EFDA, Culham Science Centre, Abingdon, Oxon, OX14 3DB, UK.”

“Enquiries about Copyright and reproduction should be addressed to the Publications Officer, EFDA, Culham Science Centre, Abingdon, Oxon, OX14 3DB, UK.”

## ABSTRACT

The (3,2) Neoclassical Tearing Mode (NTM) degrades plasma confinement by providing a region of rapid radial transport about a magnetic island structure in the plasma. As ITER is likely to be metastable to this instability it is important to understand the mechanisms of its triggering. This work is an attempt to address this question through phenomenology and statistical analysis of NTM onset data, exploring pulses both with and without the (3,2) NTM in JET ELMy H-mode plasmas. In addition to sawteeth, fishbone instabilities are observed to trigger NTMs. Both triggering instabilities have similar (1,1) mode amplitudes near the time of the (3,2) NTM onset. However, the NTM triggering does not seem to be related to the size of the magnetic precursor to the sawtooth or fishbone. For sawtooth triggered cases, the NTM probability at low  $\beta$  rises with sawtooth period. Longer sawteeth also tend to have (3,2) NTM onset at the time of the sawtooth crash, while for shorter sawtooth periods ( $\tau \leq 0.2$  s) the onset is more probable during the precursor to the crash. Many of the JET pulses analysed had both (1,1) sawtooth precursor and (1,1) fishbone bursts present at the time of the (3,2) NTM onset. The (1,1) fishbone bursts exhibit a better frequency match for forced reconnection by non-linear three wave coupling to (3,2) and (4,3) NTMs, indicating this instability to be the most likely candidate in any magnetic coupling model of NTM triggering.

## 1. INTRODUCTION

In tokamak plasmas the maximum value achievable of normalized beta,  $\beta_N \dots \beta_t \frac{I}{aB}$ , where  $\beta_t = \frac{2\mu_0 \langle p \rangle}{B^2}$  is the toroidal beta,  $B$  is the toroidal magnetic field and  $p$  is the pressure, is often limited by Magneto-HydroDynamic (MHD) modes to values below those predicted by the ideal MHD model [1]. The pressure limiting MHD instabilities are often not driven by the current gradient as a classical tearing mode [2], but by the flattening of the pressure profile over an island. This causes a helical perturbed neo-classical bootstrap current in the plasma once a seed island is sufficiently large [1, 3] and leads to an increase in the magnetic island width. Hence, these instabilities are called Neoclassical Tearing Modes (NTM).

An initial statistical study of NTM onset was made for 1999 JET experiments [4]. This work found a clear correlation between the ( $m = 3, n = 2$ ) onset and the sawtooth crash, and an approximately linear correlation between  $\beta_N$  and normalized ion Larmor radius,  $\rho_i^* = \rho_i/a$ , [5]. More recent JET experiments on controlling the NTM, by controlling the sawtooth period [6, 7], found a correlation between the onset- $\beta_N$  for NTMs and the sawtooth period. The NTM destabilised at  $\beta_N < 1$  by longer sawteeth period ( $> 400$  ms) and with shorter sawtooth period a higher  $\beta_N > 2$  is needed [6, 7, 8]. In addition the role of the sawtooth in NTM triggering has been highlighted by neural network analyses of JET data [12]. The sawtooth period was found to be the most critical parameter in predicting the time of (3, 2) NTM onset.

In the majority of cases with NBI heating the (3, 2) onset is observed clearly before the crash and during the sawtooth precursor. This suggests that the (3, 2) seed island could grow due to toroidal coupling with the  $n = 2$  component of the sawtooth precursor or through non-linear three mode

coupling [9]. In this case the, (3,2) mode would couple with a (4,3) and a (1,1) provided either by the sawtooth precursor or a fishbone burst.

In this paper we present results from a statistical analysis on the (3,2) NTM onset using a database of JET pulses between 1999 and 2002 (total of 153 pulses). The database includes ELMy H-mode regimes with ICRH or NBI heated plasmas or a combination of both. In this database the triggering of NTMs by pellets is excluded. The results are contrasted with a database with 123 pulses in ELMy H-mode regime where the (3,2) NTM was not observed.

The statistical work consists of the study on the relation between  $\beta_N$  and  $\rho^*$  at the time of the (3,2) onset; the (1,1) mode amplitude of the fishbone instabilities or sawtooth precursors nearest to the NTM onset, and other plasma parameters relevant to the NTM model (the sawtooth period and  $\beta_N$ ). In this paper we will also discuss the importance of the fishbone instability in triggering NTMs in the model of non-linear coupling.

## 2. NTM PHYSICS STUDIES

The NTM island width,  $W$ , is described by the generalized Rutherford equation [1]

$$\frac{\tau_{res}}{r_{res}} \frac{dW}{dt} = r_{res} \Delta'(W) + r_{res} \beta_p \left( a_2 \sqrt{\varepsilon} \frac{L_q}{L_p} \frac{L_q}{W^2 + W_0^2} - a_3 \frac{L_q^2}{L_p} \frac{1}{W} - a_4 g(\varepsilon, v_{ii}) \left( \rho_{pi} \frac{L_q}{L_p} \right) \frac{1}{W^3} \right) \quad (1)$$

where  $r_{res}$  is the resonant minor radius,  $\tau_{res} = \mu_0 r_{res}^2 / (1.22\eta)$  is the resistive time scale with  $\eta$  the local neoclassical resistivity,  $\Delta'$  is by definition

$$\Delta'(W) = \frac{d\psi}{dr} \Big|_{r_{res} - W/2}^{r_{res} + W/2} \frac{1}{\psi}$$

where  $\psi$  is the magnetic flux function,  $\varepsilon = r_{res}/R$  is the inverse aspect ratio of the resonant surface,  $L_q = q / \frac{dq}{dr}$  and  $L_p = p / \frac{dp}{dr}$  denote the scale lengths of the shear and pressure, respectively,  $a_2$  and  $a_3$  are the free parameters of order 1 to fit the experiment and to compensate the uncertainty of  $\Delta'$ .  $W_0$  is the minimum island width defined by  $W_0 = 5.1 (\chi_{\perp} / \chi_{\parallel})^{\frac{1}{2}} [r_{res} L_q q / (\varepsilon m)]^{\frac{1}{2}}$  [10], where  $\chi_{\perp}$  and  $\chi_{\parallel}$  are the perpendicular and parallel heat conductivity, respectively and  $m$  is the poloidal number.  $\rho_{pi}$  is the thermal ion Larmor radius defined by  $\rho_{pi} = \sqrt{2m_i T_i} / (eB_0)$ , where  $m_i$  and  $T_i$  is the ion mass and temperature in eV. The function  $g(\varepsilon, v_{ii})$  describes the influence of collisionality on the ion polarization current [5],

$$g(\varepsilon, v_{ii}) = \begin{cases} \varepsilon^{3/2}, & v_{ii}^* \ll 1 \\ 1 & v_{ii}^* \gg 1 \end{cases}$$

where,  $v_{ii}^* = v_{ii} / (m_e \omega_c^*)$ ;  $v_{ii} = \frac{n_i (Z_{\text{eff}} e)^4 \ln \Lambda_i}{12\pi^3 p \epsilon_0^2 m_i^4 T_i^3 F}$  is the ion collision frequency, is  $\omega_c^* = m \frac{T_e}{B_0 r_{\text{res}} L_p}$  the electron drift frequency and  $a_4$  is another constant adjusted to fit the experimental data. The first term on the right hand side of eq.(1) is the classical tearing mode term; the second term is the destabilizing effect from the bootstrap current; the third is the stabilizing effect due to the equilibrium pressure gradients and favourable curvature in the outer part of the island; the last term is the stabilizing effect of the polarization current.

For generalized plasma profiles and for comparison between several machines like ASDEX Upgrade, DIII-D and JET it is useful to quantify how normalized  $\beta_N$  varies with plasma parameters at the (3,2) NTM resonant surface. In the literature [5, 12] experimentally it is found that  $\beta_N$  varies approximately linearly with the normalized ion Larmor radius,  $\rho_i^* = \rho_i/a$  which is consistent with the ion polarization model amongst others. This relation in refs. 5 and 12 was derived for a limited number of pulses, with NBI only auxiliary heating. Here a larger database is considered, which includes ELMy H-mode pulses with NBI only, as well as combined NBI plus ICRH auxiliary heating. The (3,2) NTM onset maybe triggered either by sawtooth or fishbone instabilities. A plot of  $\beta_N$  versus  $\rho_i^*$  at the time of the (3,2) NTM onset is shown in figure 1 for pulses with a safety factor of  $q_{95} = 2.22 - 4.62$ , triangularity of  $\delta = 0.21 - 0.51$  and elongation of  $k = 1.54 - 1.94$ . The logarithmic linear regression fit with  $R^2 = 84\%$ , gives:

$$\beta_N = 9193.94 \rho_i^{*1.662 \pm 0.07} \quad (2)$$

In this fitting the collisionality was not considered because the collisionality dependence for JET [11] is  $\beta_N / \rho_i^{1.66} = 2.6 v_{ii}^{*-0.08}$ , and it is zero within the error bars.

For comparison in figure 2,  $\beta_N$  versus  $\rho_i^*$  at  $q = 1.5$  resonance surface radius is plotted for pulses where the NTM was not triggered. The scatter is from a wide range in  $q_{95}$  and triangularity. The time of the maximum amplitude of the (1,1) mode sawtooth precursor or fishbone instability was considered which corresponds to the time of maximum  $\beta_N$ . It is possible to observe that 69% of the pulses are above the scaling  $\beta_N$  and  $\rho_i^*$  of the (3,2) NTM onset. This leads to two conclusions; the first is that for the same value of  $\rho_i^*$  a stable NTM plasma can reach higher values of  $\beta_N$  than pulses with an NTM unstable. The second is that the scaling is a necessary condition but is not sufficient for the onset of the (3,2) NTM, as has been concluded in [12].

In the plasmas with sawteeth only it is possible to trigger the NTM at low  $\beta_N \geq 0.5$ , but with the fishbone instabilities (with or without sawteeth present) a much higher threshold  $\beta_N \geq 2.2$  must be achieved (see fig 1 and 2).

### 3. $m=1, n=1$ AMPLITUDE

Here we study the correlation between the onset  $\beta_N$  and the amplitude of the (1,1) mode (either sawtooth precursor or fishbone). The amplitude of  $m=1, n=1$  modes was obtained from observations

of magnetic field perturbations induced on magnetic pickup coils using fast Fourier transforms and filter techniques. The acquisition frequency of these coils varies from 250 kHz to 1 MHz. The spectrogram from the signal of one of these coils is shown in figure 3 for a pulse with  $I_p = 1.21$  MA,  $B_t = 1.18$  T,  $q_{95} = 3.14$ , where the (3,2) NTM was triggered before a sawtooth crash when an  $n = 1$  sawtooth pre-cursor is clearly observed. The amplitudes of the  $n=1$  and  $n=2$  modes are shown in figure 4 where it is evident that the amplitude of the sawtooth pre-cursor oscillations decrease after the (3,2) onset. In some cases the (3,2) NTM appears to be triggered by fishbones. An example is shown in figure 5 for a pulse with  $q$  on axis slightly above 1; the plasma parameters in this case are  $I_p = 1.56$  MA,  $B_t = 1.56$  T,  $q_{95} = 3.56$ . At the time of the (3,2) NTM onset the amplitude of the fishbone (1,1) component, shown in figure 6, is the same order of magnitude of the sawtooth (1,1) precursor, shown for the previous pulse in figure 4.

Pulses without the (3,2) NTM onset have also been considered. Figure 7 shows the amplitude of the (1,1) sawtooth precursor observed in a pulse with similar plasma parameters to those of the pulse shown in figure 3 ( $I_p = 1.21$  MA,  $B_t = 1.18$  T,  $q_{95} = 3.14$ ). The amplitude of the (1,1) mode is overall slightly lower than in figures 4 and 6.

For a statistical study we consider only the maximum amplitude of the (1,1) mode of the sawtooth precursor nearest to the (3,2) NTM onset and the maximum amplitude of the (1,1) mode of the fishbone instabilities at the onset. For the pulses where the (3,2) NTM onset was not observed we considered the sawtooth precursor or the fishbone instability at the time of the highest  $\beta_N$ . The (1,1) mode amplitude normalized to the poloidal magnetic field at the last flux surface radius,  $a$ , increases with increasing  $\beta_N$ , (figure 8), though there is a large scatter in data. From figure 8 it can be seen that there is no clear relation between the occurrence of the NTMs and the sawtooth precursor amplitude; this is particularly evident for  $\beta_N < 1.5$ . The lower amplitude modes are in pulses with strong ICRH heating power (figure 9). There is however a large uncertainty in the measurement of the (1,1) amplitude since for most ICRH cases with low  $\beta_N$  the sawtooth precursor is too short to be measurable.

The amplitude of the (1,1) fishbone instability at the NTM onset is of the same order as the amplitude to the (1,1) mode sawtooth precursor nearest to the onset, figure 9 (just for the cases with NTMs). Nevertheless for the same  $\beta_N$  lower fishbone amplitudes are observed at the NTM onset (figure 9) indicating that it is more probable for the NTM to be triggered by the fishbone instabilities rather than the sawtooth.

Overall for NBI heated plasmas it can be concluded that the triggering mechanism of the (3,2) NTM is not clearly related to the maximum amplitude of the (1,1). A conclusion cannot be reached for the ICRH cases.

#### 4. NTM TRIGGER RELATION WITH SAWTOOTH PERIOD

In most JET experiments for the study of the NTM onset the NBI power is ramped up. NBI power has a stabilizing effect on the sawtooth instability; increasing the power increases the sawtooth



period,  $\tau_{\text{saw}}$  [13]. Since a steady state is not reached, the period is defined by two consecutive crashes observed in the soft X-ray emission traces nearest to the time of the NTM onset. The first sawtooth crash time considered is before and the second after or at the (3,2) NTM onset, figure 3 shows an example. For the pulses without (3,2) NTM the period was determined by averaging of three consecutive sawtooth crashes with the middle one with the highest (1,1) mode amplitude. From recent experiments on JET for controlling the NTM modes by the sawtooth period [6, 7] a strong correlation between the sawtooth period and the triggering of the (3,2) NTM was found in ICRH heated discharges. Plotting the  $\tau_{\text{saw}}$  as a function of  $\beta_N$  for the larger database not triggered by the fishbone instability, figure 10, it is clear that there is no threshold for  $\tau_{\text{saw}}$  that defines stable and unstable regions. The pulses where the NTM was not observed are largely scattered with  $0.1 < \tau_{\text{saw}} < 0.6$  and  $0.7 < \beta_N < 3.0$ . Nevertheless for plasmas with  $\tau_{\text{saw}} \geq 0.6$  there is a larger probability for the onset with  $\beta_N < 1.8$ , and for shorter sawtooth periods  $\tau_{\text{saw}} \leq 0.2$  a higher  $\beta_N \geq 2$  is needed for the NTM to be destabilized. The long sawtooth periods plasmas with  $\beta_N < 1.0$  correspond in the great majority of cases to a high ICRH fraction of additional power [8], as shown in figure 11. In these plasmas with ICRH main heating the onset usually occurs at the time of the first sawtooth crash after the L to H mode transition.

The distribution of the (3,2) NTM onset time with respect to the time of the sawtooth crash for different  $\tau_{\text{saw}}$  is shown in figure 12. Correlating the time of the (3,2) NTM onset and the sawtooth crash time normalized by the sawtooth period,  $\tau_{\text{saw}}$ , it is possible to conclude that the probability is higher for the time of the onset to be before the sawtooth crash for pulses with  $\tau_{\text{saw}} < 0.3$ . For pulses with  $\tau_{\text{saw}} \geq 0.3$ , the probability is higher for the time of the onset to be at the time of the crash. This probability increases when the ICRH is used and the sawtooth period becomes longer, see figure 13. The onset before the sawtooth crash is normally in the presence of central  $n = 1$  modes (and their  $n = 2$  harmonics), figure 14. This is in accordance with the triggering of an (3,2) NTM being driven by an  $n = 1$  mode either a sawtooth precursor or a fishbone in a three-mode non-linear coupling, or by their  $n = 2$  component as the driving mode in toroidal coupling [9]. A key aspect of the three wave coupling hypothesis is the addition of these modes frequencies being approximately equal to a frequency of a third mode. In [9] it was assumed that the third mode was the (4,3) NTM mode, a nearly continuous mode observed in JET discharges at the (3,2) onset. The frequency correlation will be discussed below.

## 5. NTM MODE FREQUENCY IN RELATION TO FREQUENCY OF OTHER OBSERVED MODES AT THE ONSET

The theory described in section 2 requires a formation of a seed island above a critical value for the mode to be destabilized. In ref [9] it was proposed that this seed could be formed due to a forced reconnection of three wave non-linear coupling. In this model two modes with  $(m, n)$  and  $(m', n')$  with a frequency of  $\omega_m$  and  $\omega_{m'}$ , and phase  $\phi_m$  and  $\phi_{m'}$ , respectively can drive a third  $(m-m', n-n')$  mode with a frequency of  $\omega_{m-m', n-n'} = \omega_m - \omega_{m'}$  and phase  $\phi_{m-m', n-n'} = \phi_m - \phi_{m'}$ . In [9] the

possibility was considered that the (3,2) NTM was driven by the (1,1) sawtooth precursor and the (4,3) NTM, present at the (3,2) NTM onset. The frequencies of the MHD modes was studied for pulses with NBI heating where the (3,2) NTM onset was clearly observed before the sawtooth crash. A frequency mismatch of around 1 kHz was found in many cases [4, 9]. The fishbone instability was often observed with a higher frequency than the sawtooth precursor frequency as illustrated in figure 15. Using the (1,1) mode frequency of the fishbone at the onset, figure 16 shows that the trend line is closer to the perfect three-mode frequency match than the one from ref. [9] for the sawtooth (1,1) precursor. This indicates a stronger possibility for the three-mode coupling to occur with the fishbone oscillations rather than the sawtooth. This shows the possible importance of the fishbone instability for driving the seed island unstable. Fishbone instabilities as well as sawtooth instabilities should be taken into account when trying to control the NTM onset. An example is shown in figure 5, where the (3, 2) onset was after the sawtooth was stabilised but fishbone instability was present at the time.

Another proposal for the seed island formation was toroidal coupling of the (3,2) mode with the (2,2) mode component either provided by the sawtooth precursor or the fishbone instability. Using this theory the frequency of the (2,2) mode should match the frequency of the (3,2) NTM. In figure 17 is plotted the frequency of the (2,2) mode component versus the (3,2) mode frequency. The mismatch is worse for the fishbone (2,2) modes, than for the sawtooth precursor (2,2) component [9]. For either the sawtooth or fishbone the frequency mismatch is quite large, making this an unlikely triggering mechanism.

In the cases of ICRH pulses with long sawtooth periods, an  $n = 1$  precursor was not clearly observed before the crash. The (3,2) and (4,3) modes appear simultaneously with the sawtooth crash. It is not possible to separate the time of the onset from the crash time even when improved time-frequency analysis techniques are used [14].

## CONCLUSIONS

Using a large database with 153 JET pulses where the (3,2) NTM was observed and comparing it with a database with 123 JET pulses without the NTM leads to the following conclusions:

Pulses without the (3,2) NTM onset reached higher values of  $\beta_N$  for the same values of  $\rho^*$  when compared with pulses with NTM. The scaling between  $\beta_N$  and  $\rho^*$ ,  $\beta_N = 9193.94\rho_i^{*1.662 \pm 0.07}$  is independent on the collisionality. This scaling is a necessary condition but not a sufficient condition for the NTM to be triggered.

Fishbone instabilities as well as the sawtooth instability can trigger the (3,2) NTM. Although fishbones were observed in ICRH as well as NBI heated plasmas, fishbones were more clearly associated with the (3,2) onset in NBI heated plasmas at the higher values of  $\beta_N$  ( $\beta_N > 2.2$ ). Similar sawtooth precursor and fishbone burst amplitudes ( $\tilde{B}_b / B_p \sim 1 - 6 \times 10^{-3}$  for the (1,1) component) were observed at the time of the (3,2) NTM onset. However, for the same  $\beta_N$ , a smaller fishbone amplitude leads to the NTM onset. Overall, no sawtooth or fishbone burst threshold

amplitude has been found associated with the (3,2) NTM. A conclusion can not be reached for ICRH discharges, which have large sawtooth periods and low  $\beta_N$ , where a growing sawtooth precursor is not clearly identified.

A relevant factor in determining the time when the (3,2) NTM starts to grow is the sawtooth period, as concluded in ref [12]. The earliest NTM onsets, for  $\beta_N < 1.0$ , were observed in pulses with the longest sawtooth periods. A study of the distribution of (3,2) onset time with respect to sawtooth crash time was performed. In plasmas with long sawtooth periods,  $\tau_{\text{saw}} \geq 0.3$ , the onset is most likely to coincide with the time of the sawtooth crash. These plasmas have ICRH as additional heating sometimes combined with NBI and low  $\beta_N$  values. In plasmas with dominant NBI heating and shorter sawtooth periods,  $\tau_{\text{saw}} < 0.3$ , the onset is most probable to occur before the sawtooth crash. In the latter, the (1,1) sawtooth precursor and the (4,3) NTM mode were observed at the time of the (3,2) NTM onset. This indicates that a possible mechanism for the onset could be the three wave non-linear mode coupling [9]. In ref. [9] a mismatch of frequencies was found between these modes. In some of those pulses the fishbone instabilities were present. The fishbone has a higher mode frequency than the sawtooth precursor decreasing the three-mode frequency mismatch. Thus in NBI heated pulses, the fishbone instability is more likely than the sawtooth precursor to trigger the (3,2) NTM by non-linear three-mode coupling.

The mismatch of frequencies between the (2,2) mode component of the fishbone or the sawtooth precursor and the (3,2) NTM mode is large. Thus two mode toroidal coupling is a less probable mechanism for the onset.

## ACKNOWLEDGEMENTS

This work, which has been supported by the European Communities and the Instituto Superior T cnico (IST) under the Contract of Association between the European Atomic Energy Community and IST, was performed under the European Fusion Development Agreement. The views and opinions expressed herein do not necessarily reflect those of the European Commission and IST.

## REFERENCES

- [1]. Sauter, O., *et al*, Phys. Plasmas, **4** (1997) 1654.
- [2]. Rutherford, R.H., Phys. Fluids, **16** (1980), 1903
- [3]. Wilson, H.R., Connor, J.W., Hastie, R.J., Hegna, C.C., Phys. Plasmas **3**, (1996) 248.
- [4]. Buttery, R.J., *et al*, Nuclear Fusion **43** (2003) 69
- [5]. La Haye, R. J., *et al*, Phys. Plasma **7** (2000) 3349
- [6]. Sauter, O., *et al*, Phys. Rev. Letters, **88** (2002) 105001
- [7]. Westerhof, E., *et al*, Nuclear Fusion **42** (2002) 1324
- [8]. Hender, T.C., IAEA-CN-94 EX/S1-2 (2002)
- [9]. Nave, M.F.F., *et al*, Nuclear Fusion **43** (2003) 179
- [10]. Fitzpatrick, R., Phys. Plasma **2** (1995) 825

- [11]. Buttery, R.J., *et al*, Plasma Phys. Contr. Fusion **42** (2000) B61
- [12]. Buttery, R.J., *et al*, Nuclear Fusion, **44** (2004) 678
- [13]. Angioni, C. *et al*, Plasma Phys. Contr. Fusion **44** (2002) 205
- [14]. Figueireido, J.A., Nave, M.F.F., Proceeding 30<sup>th</sup> EPS, San Petersburg, 2003

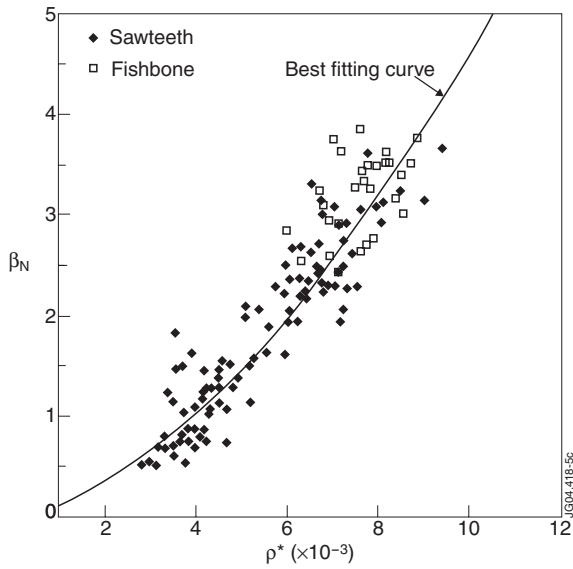


Figure 1:  $\beta_N$  values in function of  $\rho_i^*$  at the (3,2) NTM onset.

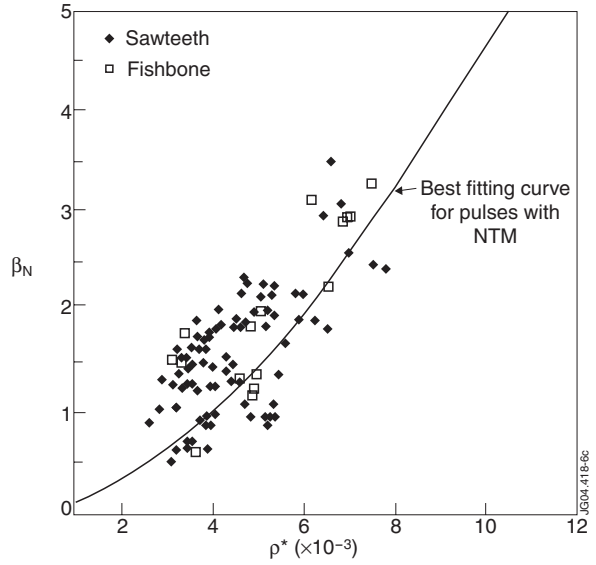


Figure 2:  $\beta_N$  values in function of  $\rho_i^*$  at the maximum (1,1) amplitude of the sawtooth precursors and fishbone instability for pulses where an NTM was not triggered

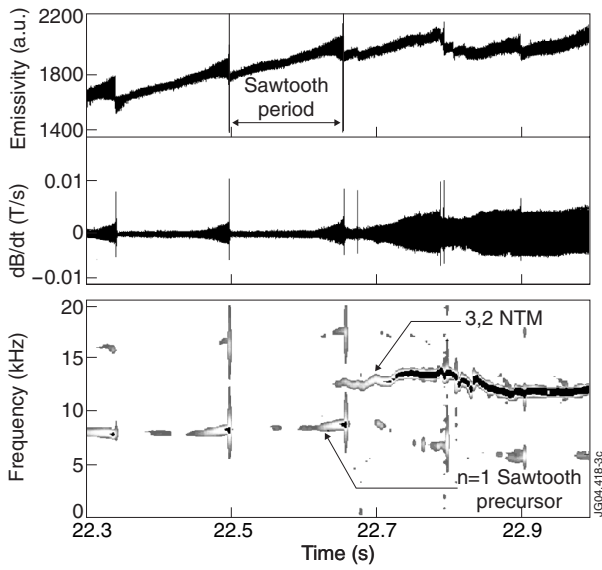


Figure 3: Signal from the Soft X-ray central emission, induced signal in a fast pickup coil from the Pulse No: 51995 and the correspondent spectrogram showing a (3, 2) NTM triggered shortly before a sawtooth crash.

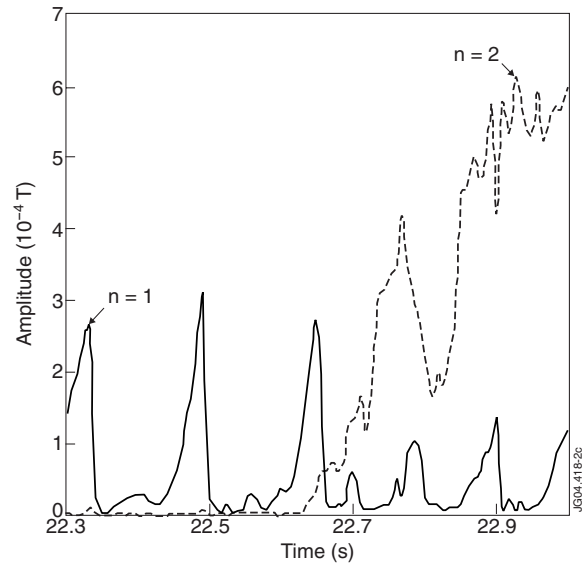


Figure 4: Amplitudes of the  $n=1$  sawtooth precursor and  $n=2$  NTM mode for the Pulse No: 51995.

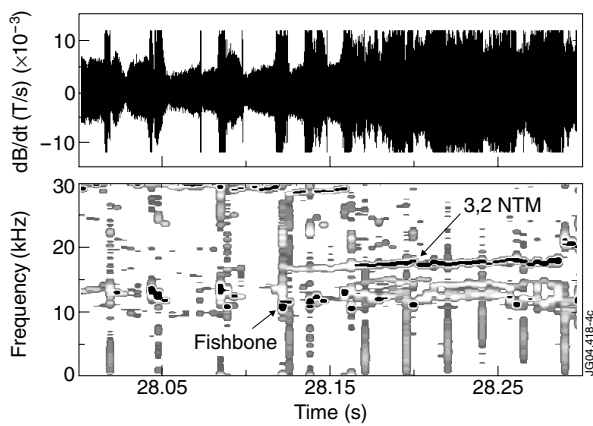


Figure 5: Induced Signal in a fast pickup coil from the Pulse No: 52083 and its correspondent spectrogram showing a NTM triggered in a discharge with frequent fishbones

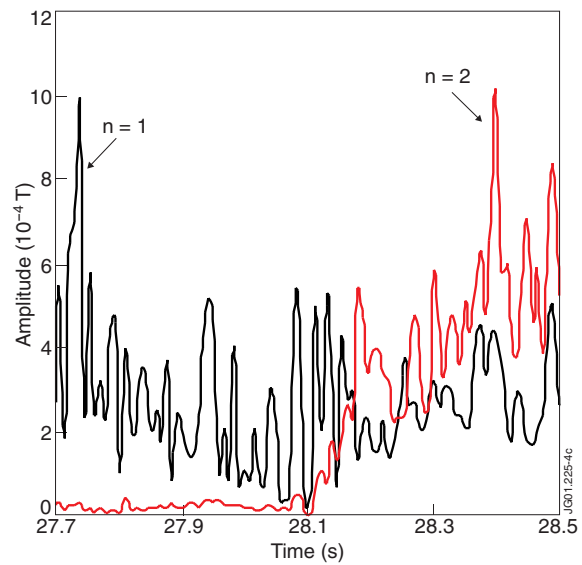


Figure 6: Amplitude of the  $n=1$  fishbone bursts and  $n=2$  NTM modes for the Pulse No: 52083

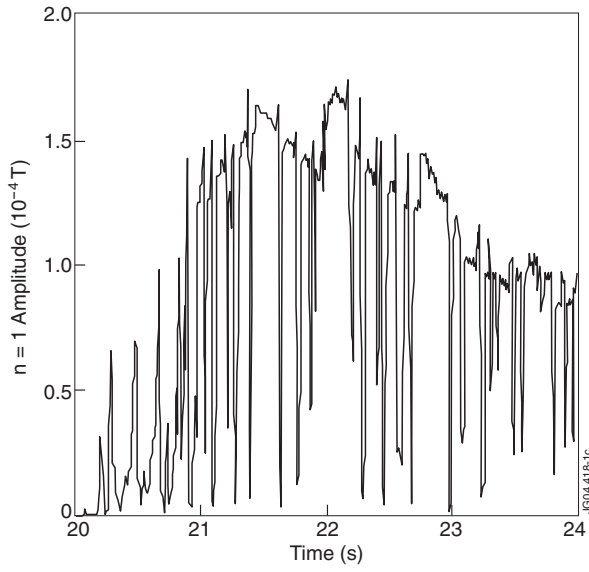


Figure 7: Amplitude of the  $n=1$  sawtooth precursor mode for the Pulse No: 52002 where a NTM was not found

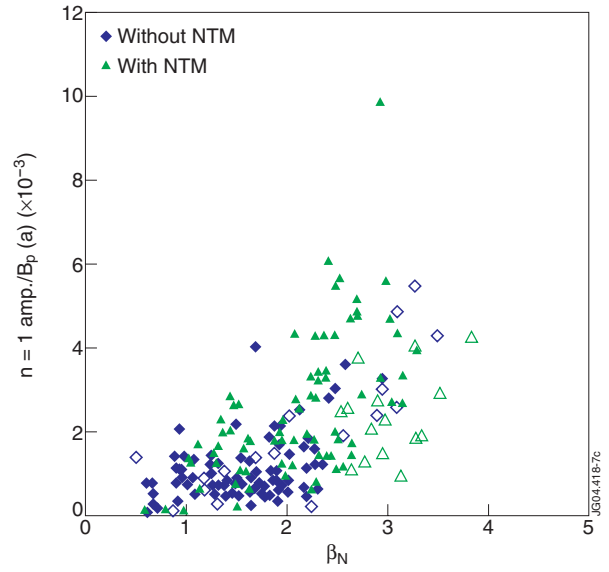


Figure 8: Amplitude of the  $m=1, n=1$  sawtooth precursor (filled symbols) and the fishbone (open symbols) normalised by  $B_p$  at its maximum amplitude versus  $\beta_N$ , for pulses where the (3,2) NTM was observed (green triangles) and was not observed (blue diamonds). For the latter the time of  $\beta_N$  max was considered.

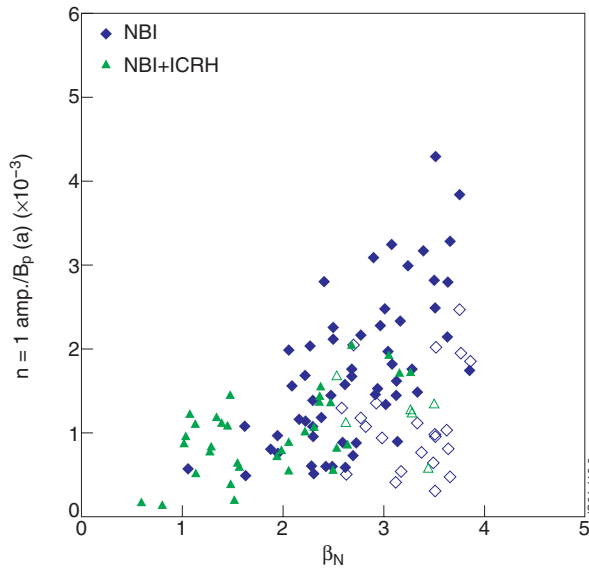


Figure 9: Amplitude of the  $m=1, n=1$  sawtooth precursor (filled symbols) and the fishbone (open symbols) normalised by  $B_p$  versus  $\beta_N$ , for pulses with NBI only (blue diamonds) and with ICRH (green triangles) for pulses with NTMs. The amplitude of the (1,1) fishbone at the NTM onset is on average lower than the amplitude of the sawtooth precursor for similar  $\beta_N$

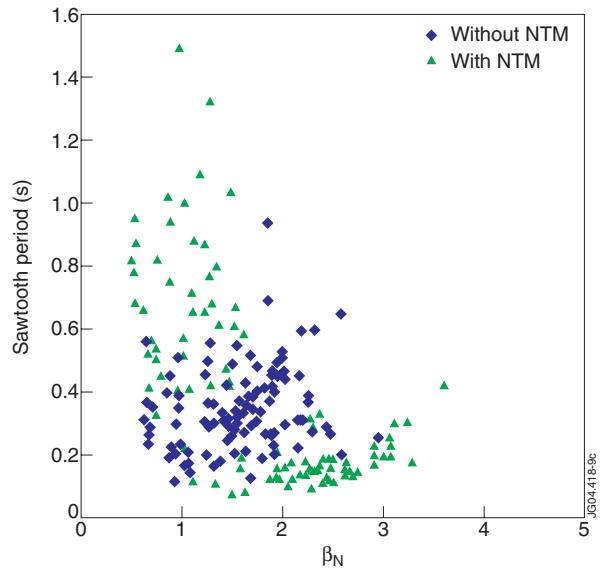


Figure 10:  $\beta_N$  versus sawtooth period without fishbone instabilities at the  $\beta_N$ .

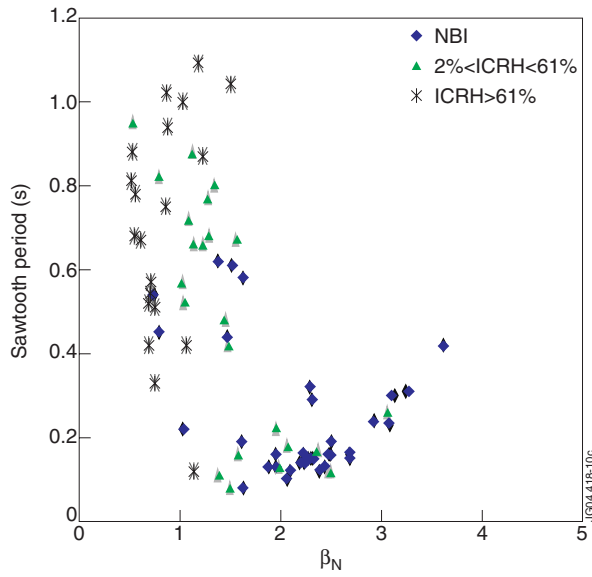


Figure 11:  $\beta_N$  versus sawtooth period without fishbone instabilities at the NTM onset.

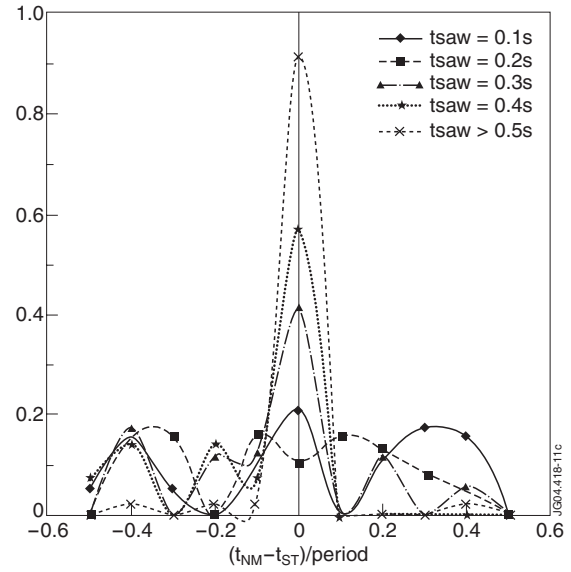


Figure 12: Probability distribution of (3,2) NTM occurrence for pulses with different sawtooth period.

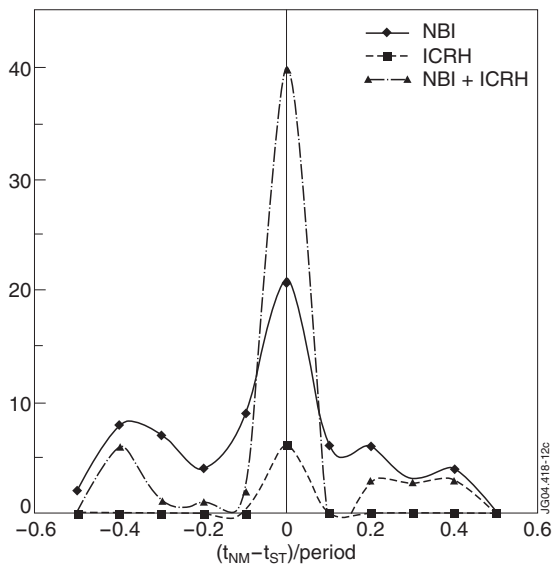


Figure 13: Distribution of NTM occurrence with: NBI only additional heating (continues line); ICRH only additional heating (dashed line); combined additional heating of NBI and ICRH (dashed and dotted line).

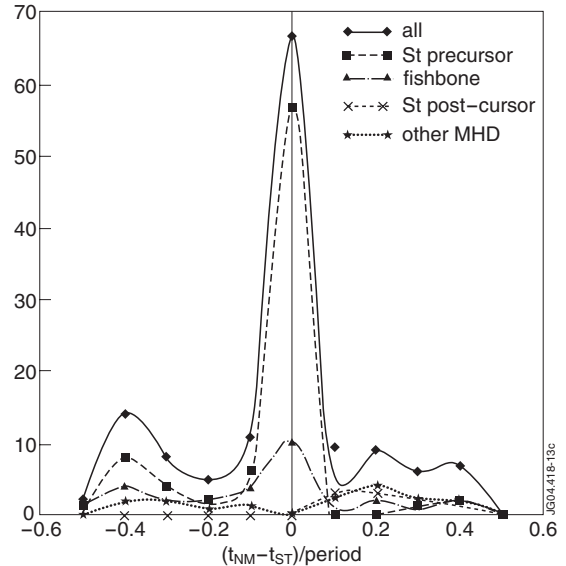


Figure 14: Distribution of NTM occurrence (129 pulses) with respect to the nearest sawtooth crash (continues line). Distribution of cases occurring when: a sawtooth precursor is observed (dashed line); fishbones are present (dashed and dotted line);  $n=1$  sawtooth post-cursor (dotted line with crosses).

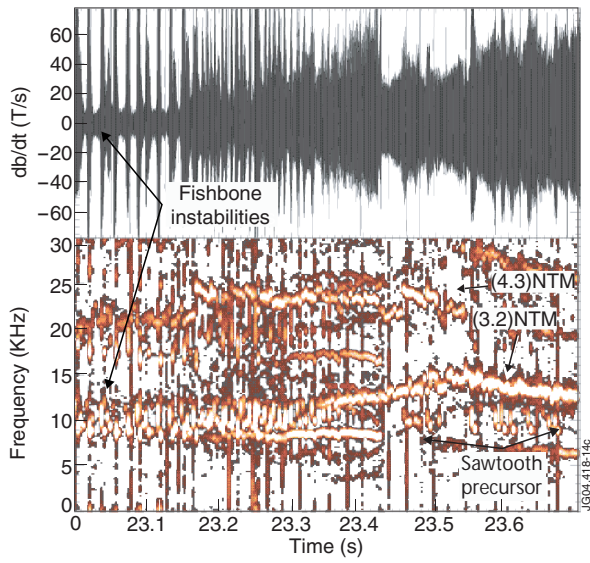


Figure 15: Magnetic signal and its spectrogram from Pulse No: 52071. At the (3,2) NTM onset the (1,1) modes of the fishbone instability and of the sawtooth precursor were present.

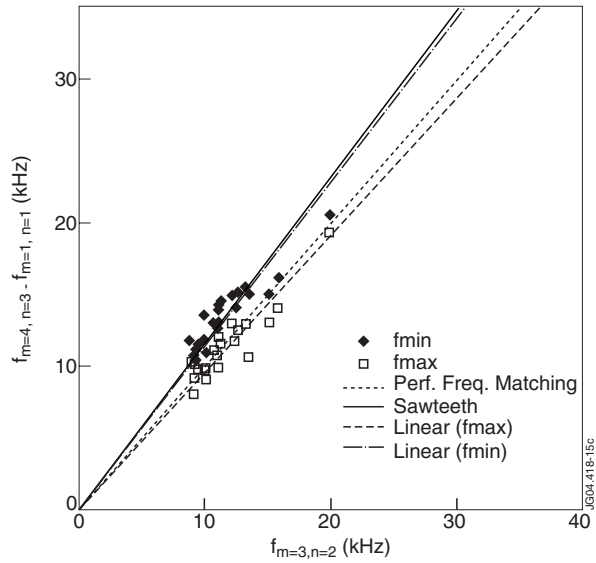


Figure 16: Frequency of the (3,2)NTM versus the difference between the frequency of the (3,2) mode and the maximum (open symbols) and minimum (close symbols) frequencies of the fishbone instabilities. The trend line from the ref. [9] related to the sawtooth (full line) and the line of perfect frequency matching (dotted line).

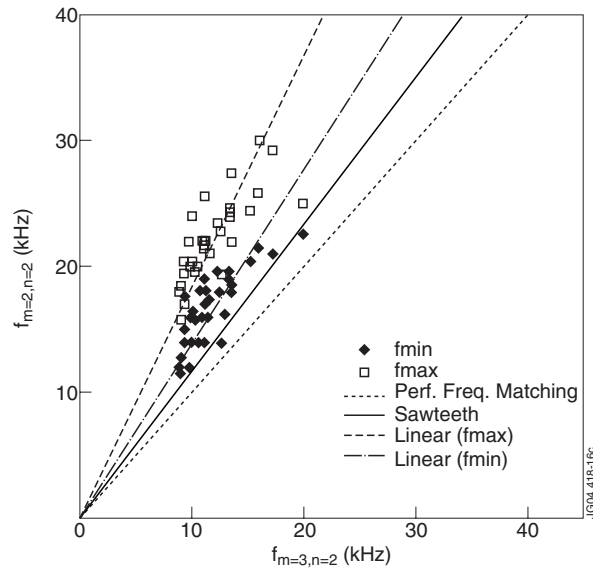


Figure 17: Maximum and minimum frequencies of the  $n=2$  second harmonic of the fishbone instabilities versus the  $n=2$  mode frequency. The trend line from the ref. [9] related to the sawtooth (full line) and the line of perfect frequency matching (dotted line).